The degradation of phenol *via in situ* H$_2$O$_2$ production over supported Pd-based catalysts†

Alba Santos,‡[a] Richard J. Lewis, ‡*[a] David J. Morgan, [ab] Thomas E. Davies,[a] Euan Hampton,[c] Paul Gaskin[c] and Graham J. Hutchings *[a]

The oxidative degradation of phenol *via* the *in situ* production of H$_2$O$_2$ from molecular H$_2$ and O$_2$ offers an attractive route to the destruction of organic contaminants in water streams, potentially overcoming the significant economic and environmental concerns associated with traditional water remediation technologies. Herein we demonstrate the efficacy of a series of bifunctional Pd-based catalysts, which offer appreciable rates of phenol degradation. In particular, the introduction of Fe into a supported Pd catalyst leads to a near four-fold increase in pollutant remediation. We ascribe this improvement in catalytic performance to the ability of Fe to catalyse the formation of oxygen-based radical species from *in situ* synthesised H$_2$O$_2$ *via* Fenton's pathways and the promotion of Pd domains of mixed oxidation state, with a resulting inhibition of H$_2$O$_2$ degradation pathways.

Introduction

A major challenge of the coming decades will revolve around access to potable water, with increased competition driven largely by a combination of population growth, urbanisation and industrialisation. With the most severe risks effecting communities that are already facing water-scarcity and those who are not currently served by traditional water disinfection infrastructure, which typically relies on chlorination. As such there is a pressing need to develop alternative means of water treatment, with a particular focus on decentralized approaches.[1] In particular there is a growing concern around the environmental and health impacts of organic pollutants released from industrial, agricultural and urban activities, including dyes, pharmaceuticals and pesticides.[2]

The high resistance of many organic compounds found in industrial waste streams to conventional chemical or biological treatments has led to growing interest in the application of advanced oxidation processes (AOPs), which utilise oxygen-based radicals, primarily hydroxyl radicals (˙OH), for contaminant degradation.[3] In particular the combination of pre-formed H$_2$O$_2$ with ozone (O$_3$/H$_2$O$_2$) or ultraviolet light (UV/H$_2$O$_2$) offers an attractive route to the remediation of such recalcitrants. However, the high costs associated with reagents such as O$_3$ or H$_2$O$_2$ or indeed with energy light sources have precluded their application on an industrial scale.[4] Similarly, the generation of ˙OH radials from H$_2$O$_2$ *via* the use of Fenton's reagents, typically homogenous Fe^{2+} species,[5] has suffered from the need to remove Fe or other Fenton-like metals from waste streams. In addition, there is a need to maintain a low pH to achieve optimal catalytic performance with such approaches.[6] Which, when coupled with the additional costs associated with the neutralisation and purification of treated waste streams prior to discharge are likely to preclude the application of such approaches on a meaningful scale.[7]

Furthermore, there are added complications associated with the use of pre-formed H$_2$O$_2$. These largely result from the means by which H$_2$O$_2$ is generated on an industrial scale, the anthraquinone oxidation (AO) process. While highly efficient, economies of scale in addition to the complexity of the AO process preclude the production of H$_2$O$_2$ on-site *via* this route. As such H$_2$O$_2$ is typically transported and stored at concentrations (30–70 wt%) greatly exceeding that required by the end user (typically 1–10 wt%), prior to dilution, with this effectively wasting the energy utilised in the concentration process.[8] Additionally, the low stability of H$_2$O$_2$, readily decomposing to H$_2$O under mild temperatures or weakly basic conditions necessitates the use of acidic or halide stabilizing agents to prolong shelf-life.[9] While effective in promoting H$_2$O$_2$ stability, the presence of such agents not only lead to reactor corrosion but also present a hazard to human and aquatic life.[10] As such, if such processes were

[a] *Max Planck Centre for Fundamental Heterogeneous Catalysis (FUNCAT), Cardiff Catalysis Institute, School of Chemistry, Cardiff University, Main Building, Park Place, Cardiff, CF10 3AT, UK. E-mail: LewisR27@Cardiff.ac.uk, Hutch@Cardiff.ac.uk*
[b] *HarwellXPS, Research Complex at Harwell (RCaH), DidcotOX11 OFA, UK*
[c] *Dŵr Cymru Welsh Water, Pentwyn Road, Nelson, Treharris, CF46 6LY, UK*
† Electronic supplementary information (ESI) available. See DOI: 10.1039/d1cy01897c
‡ These authors contributed equally to this work.

7866 | *Catal. Sci. Technol.*, 2021, **11**, 7866–7874

This journal is © The Royal Society of Chemistry 2021

adopted for potable water treatment additional costly purification steps would be required to ensure their removal prior to the discharge of the treated water.

The *in situ* synthesis of H_2O_2 from molecular H_2 and O_2 offers an attractive alternative to the use of pre-formed H_2O_2, overcoming the considerable aforementioned concerns. In particular the activity of Pd catalysts towards H_2O_2 production has been well established.[8,11,12] However, due to limited selectivity there is often a need to alloy Pd with a range of precious metals,[13–17] although in recent years, a growing attention has been placed on the use of more abundant transition metals as promoters for Pd.[18–23] Indeed, we have recently demonstrated the ability of bi-functional Pd-based bimetallic nanoparticles to catalyse the direct synthesis of H_2O_2 in addition to the selective oxidation of a range of substrates[24–26] as well as the remediation of microorganisms through radical pathways.[27] With these studies in mind, we now investigate the efficacy of supported Pd-based bimetallic catalysts that combine the H_2O_2 synthesising activity of Pd and the ability of a range of transition metals to generate reactive oxygen species through Fenton's pathways for the degradation of phenol.

Experimental

Catalyst synthesis

Mono- and bi-metallic 1% PdX/TiO$_2$ (X = Au, Fe, Co, Cu) catalysts, prepared on a weight basis, with a Pd : X ratio of 1 : 1 (wt/wt) have been synthesised *via* an excess chloride co-impregnation procedure, based on methodology previously reported in the literature.[28,29] With catalysts produced *via* an impregnation procedure widely studied for the direct synthesis of H_2O_2 due to the simplicity and ease with which this approach can be scaled to meet industrial application. In particular catalysts prepared *via* the excess chloride co-impregnation route, where precious metal precursors (in this case the PdCl$_2$) are acidified with HCl (0.58 M) have been shown to offer enhanced performance in a range of chemical transformations, including the direct synthesis of H_2O_2, compared to analogous materials prepared *via* a conventional wet co-impregnation procedure, where the metal precursors are not highly acidified.[28] This has been attributed to a combination of improved alloy formation and enhanced nanoparticle dispersion.

The procedure to produce 0.5% Pd–0.5% Fe/TiO$_2$ (2 g) is detailed below, with a similar methodology utilized for all mono- and bi-metallic catalysts using chloride-based metal precursors in all cases (see Table S.1† for further details). In all cases catalysts have been prepared using PdCl$_2$ (0.58 M HCl, 6 mg mL^{-1}, Merck).

Aqueous acidified PdCl$_2$ solution (1.667 mL, 0.58 M HCl, 6 mg mL^{-1}, Merck) and aqueous FeCl$_3$·6H$_2$O solution (0.0484 mL, 6 mg mL^{-1}, Merck) were mixed in a 50 mL round-bottom flask and heated to 65 °C with stirring (1000 rpm) in a thermostatically controlled oil bath, with total volume fixed to 16 mL using H$_2$O (HPLC grade). Upon reaching 65 °C,

TiO$_2$ (1.98 g, Degussa, P25) was added over the course of 5 min with constant stirring. The resulting slurry was stirred at 65 °C for a further 15 min, following this the temperature was raised to 95 °C for 16 h to allow for complete evaporation of water. The resulting solid was ground prior to a reductive heat treatment (5% H$_2$/Ar, 400 °C, 4 h, 10 °C min^{-1}).

Total metal loading, as determined by MP-AES analysis of *aqua regia* digested catalysts can be seen in Table S.2,† with the corresponding surface area measurements, as determined by five-point N$_2$ adsorption in Table S.3.†

Catalyst testing

Note 1. Reaction conditions used within this study operate below the flammability limits of gaseous mixtures of H$_2$ and O$_2$.

Note 2. The conditions used within this work for H_2O_2 synthesis and degradation have previously been investigated, where the presence of CO$_2$ as a diluent for reactant gases, methanol co-solvent and sub-ambient reaction temperatures have been identified as key to maintaining high catalytic efficacy towards H_2O_2 production.[29] In particular we have previously demonstrated that the use of the CO$_2$ diluent can greatly enhance H_2O_2 stability through the formation of carbonic acid *in situ*. Indeed, the effect of CO$_2$ has been shown to be comparable to that achieved through the addition of HNO$_3$ to the reaction solution, so that the pH was reduced to a value of 4.[30] However, unlike the use of halo- or oxo-acid stabilisers the formation of carbonic acid *in situ* would not necessitate additional costly seperation steps.

Direct synthesis of H_2O_2

Hydrogen peroxide synthesis was evaluated using a Parr Instruments stainless steel autoclave with a nominal volume of 50 mL, equipped with a glass liner so that nominal volume is reduced to 33 mL, and a maximum working pressure of 2000 psi. To test each catalyst for H_2O_2 synthesis, the autoclave liner was charged with catalyst (0.01 g) and solvent (8.5 g H$_2$O, HPLC Grade, Fischer Scientific). The charged autoclave was then purged three times with 5% H$_2$/CO$_2$ (100 psi) before filling with 5% H$_2$/CO$_2$ to a pressure of 420 psi, followed by the addition of 25% O$_2$/CO$_2$ (160 psi). Pressure of 5% H$_2$/CO$_2$ and 25% O$_2$/CO$_2$ are given as gauge pressures. The reaction was conducted at a temperature of 2 °C, for 0.5 h with stirring (1200 rpm). H_2O_2 productivity was determined by titrating aliquots of the final solution after reaction with acidified Ce(SO$_4$)$_2$ (0.0085 M) in the presence of ferroin indicator. Catalyst productivities are reported as mol$_{H_2O_2}$ kg$_{cat}^{-1}$ h^{-1}. Reactant gases were not continually supplied.

Reactor temperature was controlled using a HAAKE K50 bath/circulator using an appropriate coolant.

Similar reactions were carried out under reaction conditions identical to those used for the oxidative degradation of phenol *via in situ* H_2O_2 synthesis, namely in the absence of the methanol co-solvent and at 30 °C.

Degradation of H₂O₂

Catalytic activity towards H₂O₂ degradation (*via* hydrogenation and decomposition pathways) was determined in a similar manner to the direct synthesis activity of a catalyst. The autoclave liner was charged with water (7.81 g, HPLC grade, Fischer Scientific), H₂O₂ (50 wt% 0.69 g, Merck), and catalyst (0.01 g), with the solvent composition equivalent to a 4 wt% H₂O₂ solution. From the solution 2 aliquots of 0.05 g were removed and titrated with acidified $Ce(SO_4)_2$ solution using ferroin as an indicator to determine an accurate concentration of H₂O₂ at the start of the reaction. The autoclave was pressurised with 420 psi 5% H₂/CO₂ (gauge pressure). The reaction was conducted at a temperature of 2 °C, for 0.5 h with stirring (1200 rpm). After the reaction was complete the catalyst was removed from the reaction mixture and two aliquots of 0.05 g were titrated against the acidified $Ce(SO_4)_2$ solution using ferroin as an indicator. The degradation activity is reported as $mol_{H_2O_2}$ kg_{cat}^{-1} h^{-1}.

Similar reactions were carried out under reaction conditions identical to those used for the oxidative degradation of phenol *via in situ* H₂O₂ synthesis, namely in the absence of the methanol co-solvent and at 30 °C.

Oxidative degradation of phenol *via* the *in situ* production of H₂O₂

Catalytic activity towards the degradation of phenol was evaluated using a Parr Instruments stainless steel autoclave with a nominal volume of 50 mL, equipped with a glass liner so that nominal volume is reduced to 33 mL, and a maximum working pressure of 2000 psi. In a typical test the autoclave was charged with catalyst (0.01 g) and phenol (8.5 g, 1000 ppm aqueous phenol). The charged autoclave was then purged three times with 5% H₂/CO₂ (100 psi) before filling with 5% H₂/CO₂ to a pressure of 420 psi, followed by the addition of 25% O₂/CO₂ (160 psi). Pressure of 5% H₂/CO₂ and 25% O₂/CO₂ are given as gauge pressures. The reactor was then heated to 30 °C followed by stirring (1200 rpm) typically for 2 h. After 2 h gas mixtures were sampled and analysed *via* GC (Varian 3800 GC fitted with a TCD and equipped with a Porapak Q column). The reaction solution was collected and catalyst removed *via* filtration, the post-reaction solution was analysed by high performance liquid chromatography (HPLC) fitted with an Agilent Poroshell 120 SB-C18 column. Reactant gases were not continually supplied.

Throughout product distribution is of phenol oxidation have been grouped into two categories, namely phenol oxygenated derivatives (catechol, hydroquinone *etc.*) and organic acids (oxalic acid, formic acid *etc.*). While it is theoretically possible for the completed oxidation of phenol to occur, the presence of water as a reaction medium and carbon dioxide as a reagent gas diluent prevents the detection of these total oxidation products.

Phenol conversion (eqn (1)), H₂ conversion (eqn (2)) and selectivity towards phenolic derivatives (eqn (3)) or organic acids (eqn (4)) are defined as follows:

$$\text{Phenol Conversion (\%)} \qquad (1)$$
$$= \frac{\text{mmol}_{\text{phenol}(t(0))} - \text{mmol}_{\text{phenol}(t(1))}}{\text{mmol}_{\text{phenol}(t(0))}} \times 100$$

$$\text{H}_2 \text{ Conversion (\%)} = \frac{\text{mmol}_{\text{H}_2(t(0))} - \text{mmol}_{\text{H}_2(t(1))}}{\text{mmol}_{\text{H}_2(t(0))}} \times 100 \qquad (2)$$

$$\text{Selectivity}_{\text{phenolic derivitives}} \text{ (\%)} \qquad (3)$$
$$= \frac{\text{Phenolic derivitives observed (mmol)}}{\text{Phenol consumed (mmol)}} \times 100$$

$$\text{Selectivity}_{\text{organic acids}} \text{ (\%)} \qquad (4)$$
$$= \frac{\text{mmol}_{\text{phenol}(t(1))} - \text{mmol}_{\text{phenol derivatives}(t(1))}}{\text{mmol}_{\text{phenol}(t(0))}}$$

Catalytic hydrogenation of phenol

In order to determine the ability of the Pd-based catalysts to convert phenol to hydrogenation products under *in situ* oxidation reaction conditions an identical procedure to that outlined above for the for the degradation of phenol was followed for a reaction time of 2 h, with the 25% O₂/CO₂ component typically used exchanged for N₂ (160 psi).

Gas replacement experiments for the oxidative degradation of phenol *via* the *in situ* production of H₂O₂

An identical procedure to that outlined above for the degradation of phenol was followed for a reaction time of 2 h. After this, stirring was stopped and the reactant gas mixture was vented prior to replacement with the standard pressures of 5% H₂/CO₂ (420 psi) and 25% O₂/CO₂ (160 psi). The reaction mixture was then stirred (1200 rpm) for a further 2 h. To collect a series of data points, as in the case of Fig. 2, it should be noted that individual experiments were carried out and the reactant mixture was not sampled on-line.

Hot filtration experiments for the oxidative degradation of the oxidation of phenol *via* the *in situ* production of H₂O₂

An identical procedure to that outlined above for the oxidative degradation of phenol was followed for a reaction time of 1 h. Following this, the stirring was stopped, and the reactant gas mixture vented prior to the removal of the solid catalyst *via* filtration. The post-reaction solution was returned to the reactor to identify the contribution of leached species to the observed activity, with both steps of the reaction conducted at a temperature of 30 °C. Further experiments were conducted, where a fresh 1% Pd/TiO₂ catalyst (0.01 g) or preformed H₂O₂, comparable to that if all the H₂ converted in the first 1 h reaction was converted selectively to H₂O₂, was added to the reaction mixture prior to running the reaction for a further 1 h.

Catalyst characterisation

A Thermo Scientific K-Alpha⁺ spectrometer was used to collect X-ray photoelectron spectra utilizing a microfocused

7868 | *Catal. Sci. Technol.*, 2021, **11**, 7866–7874

This journal is © The Royal Society of Chemistry 2021

monochromatic Al Kα X-ray source operating at 72 W (6 mA × 12 kV). Data were collected over a X-ray spot defined elliptical area with a radius of approximately 400 μm^2 at pass energies of 40 and 150 eV for high-resolution and survey spectra, respectively. Sample charging effects were minimized through a combination of low-energy electrons and Ar$^+$ ions, and a C(1s) line at 284.8 eV was present for all samples. All data were processed using CasaXPS v2.3.24 (ref. 31) using a Shirley background, Scofield sensitivity factors, and an electron energy dependence of −0.6. Fitting was achieved using models taken from bulk compounds (Pd and Au metal foils and PdO). The Au(4f) peaks fit on top of the Ti loss structure and also the Pd(4s) signal; to account for this background, a broad, constrained Voight function was used to model these underlying peaks.

The bulk structure of the catalysts was determined by powder X-ray diffraction using a (θ–θ) PANalytical X'pert Pro powder diffractometer using a Cu K$_α$ radiation source, operating at 40 KeV and 40 mA. Standard analysis was carried out using a 40 min run with a back filled sample, between 2θ values of 10–80°. Phase identification was carried out using the International Centre for Diffraction Data (ICDD).

Transmission electron microscopy (TEM) was performed on a JEOL JEM-2100 operating at 200 kV. Samples were prepared by dispersion in ethanol by sonication and deposited on 300 mesh copper grids coated with holey carbon film. Energy dispersive X-ray analysis (EDX) was performed using an Oxford Instruments X-Max^N 80 detector and the data analysed using the Aztec software.

Total metal loading and metal leaching from catalyst supported was quantified using microwave plasma – atomic emission spectroscopy (MP-AES). Fresh catalysts were digested (25 mg catalyst, 2.5 ml *aqua regia*, 24 h) prior to analysis using an Agilent 4100 MP-AES, while post reaction solutions were also analysed after filtration of the solid material. The concentration of leached metals in product streams was quantified through microwave plasma atomic emission spectroscopy (MP-AES) using an Agilent MP-AES 4100. Post-reaction solutions were filtered using PTFE syringe filters (0.45 μm) prior to analysis for Fe and Pd. Emission lines were calibrated using commercial standards (Merck), in all cases $r^2 > 0.999$.

Brunauer–Emmett–Teller (BET) surface area measurements were conducted using a Quadrasorb surface area analyzer. A five-point isotherm of each material was measured using N$_2$ as the adsorbate gas. Samples were degassed at 250 °C for 2 h prior to the surface area being determined by five-point N$_2$ adsorption at −196 °C, and data were analyzed using the BET method.

^{1}H NMR spectra were recorded on a Bruker Ultrashield 500 MHz spectrometer, using a H$_2$O solvent suppression program. Filtered post-hydrogenation reaction solvent (0.7 mL) was added to an NMR tube containing D$_2$O (0.1 mL). In a similar manner cyclohexanone and cyclohexanol standards (0.7 mL, both Merck) were added to an NMR tube containing CDCl$_3$ (0.1 mL, Merck).

Results and discussion

Our initial studies investigated the efficacy of a range of supported bimetallic catalysts, prepared by a co-impregnation, excess chloride procedure towards the direct synthesis and subsequent degradation of H$_2$O$_2$ (Table 1). These experiments were carried out under conditions previously optimised to enhance H$_2$O$_2$ stability, namely in the presence of a methanol co-solvent, CO$_2$ gaseous diluent and sub-ambient reaction temperatures, all of which have been shown to inhibit H$_2$O$_2$ degradation pathways.[29]

In keeping with numerous studies,[32–34] the introduction of Au into a supported Pd catalyst was found to significantly improve catalytic performance towards H$_2$O$_2$ synthesis, with H$_2$O$_2$ synthesis rates (97 mol$_{H_2O_2}$ kg$_{cat}^{-1}$ h^{-1}) far greater than that observed over the Pd-only catalyst (30 mol$_{H_2O_2}$ kg$_{cat}^{-1}$ h^{-1}). The introduction of a range of secondary base-metals, (Fe, Cu, Co) which are well-known to catalyse H$_2$O$_2$ decomposition to H$_2$O *via* Fenton pathways[35] offered lower H$_2$O$_2$ synthesis to that observed for the PdAu analogue, although with the exception of the 0.5% Pd–0.5% Cu/TiO$_2$ catalyst, rates of H$_2$O$_2$ synthesis were comparable to the 1% Pd/TiO$_2$ catalyst. Interestingly, the introduction of Fenton or Fenton-like metals did not result in an enhancement in activity towards H$_2$O$_2$ degradation (*via* hydrogenation or decomposition pathways), which may have been expected, with these materials offering H$_2$O$_2$ degradation rates significantly lower than either the PdAu (258 mol$_{H_2O_2}$ kg$_{cat}^{-1}$ h^{-1}) or Pd-only catalysts (198 mol$_{H_2O_2}$ kg$_{cat}^{-1}$ h^{-1}). This is in keeping with our previous studies[24,36] and may be ascribed to a combination of (i) the reaction conditions chosen to

Table 1 Catalytic performance of Pd-based bi-metallic catalysts towards the direct synthesis and subsequent degradation of H$_2$O$_2$

Catalyst	Productivity/mol$_{H_2O_2}$ kg$_{cat}^{-1}$ h^{-1}	Degradation/mol$_{H_2O_2}$ kg$_{cat}^{-1}$ h^{-1}
1% Pd/TiO$_2$	30	198
0.5% Pd–0.5% Au/TiO$_2$	97	258
0.5% Pd–0.5% Cu/TiO$_2$	11	80
0.5% Pd–0.5% Co/TiO$_2$	42	109
0.5% Pd–0.5% Fe/TiO$_2$	38	51

H$_2$O$_2$ direct synthesis reaction conditions: catalyst (0.01 g), H$_2$O (2.9 g), MeOH (5.6 g), 5% H$_2$/CO$_2$ (420 psi), 25% O$_2$/CO$_2$ (160 psi), 0.5 h, 2 °C, 1200 rpm. H$_2$O$_2$ degradation reaction conditions: catalyst (0.01 g), H$_2$O$_2$ (50 wt% 0.68 g) H$_2$O (2.22 g), MeOH (5.6 g), 5% H$_2$/CO$_2$ (420 psi), 0.5 h, 2 °C, 1200 rpm.

This journal is © The Royal Society of Chemistry 2021

Catal. Sci. Technol., 2021, **11**, 7866–7874 | **7869**

determine H_2O_2 synthesis and degradation activity, with the dissolution of the CO_2 reactant gas diluent forming carbonic acid *in situ*, resulting in H_2O_2 stabilisation[30] or (ii) the possible modification of Pd oxidation state as a result of secondary metal introduction. With the formation of mixed domains, consisting of Pd^0 and Pd^{2+} well reported to offer enhanced catalytic performance towards H_2O_2 synthesis, compared to purely Pd^0 or Pd^{2+} analogues.[14,37] However, our analysis by XPS (Fig. S.1†) reveals that while the introduction of base-metals (Fe, Cu, Co) does enhance Pd^{2+} content, a similar shift in Pd speciation is similarly observed with the introduction of Au, and as such we cannot definitively attribute the enhanced catalytic H_2O_2 synthesis activity of the Pd-X (Fe, Cu, Co) catalysts to the increased presence of Pd^0–Pd^{2+} species. It should be noted that a number of previous experimental[38,39] and computational[40] studies have revealed the ability of high concentrations of Cu to inhibit catalytic activity towards H_2O_2 production. Indeed, Joshi *et al.* have revealed the thermodynamic instability of intermediate hydroperoxyl (OOH*) species and in turn H_2O_2 over Cu-containing surfaces.[40]

The generation of hydroxyl radicals *via* Fenton's or photo-Fenton's pathways has been well reported to offer high efficacy in the remediation of organic contaminants,[41–43] with this in mind we next investigated the efficacy of these Pd-based bi-metallic catalysts towards the oxidative degradation of phenol *via in situ* H_2O_2 production (Table 2). It should be noted that it was not possible to measure residual H_2O_2 *via* standard titration or colorimetric procedures given the strong reddish colour that results from the formation of the aromatic oxidation products (catechol, hydroquinone *etc.*).[44] However, our previous studies have determined the ability of H_2O_2 to be synthesised under reaction conditions comparable to those used within this study.[45]

Interestingly, a direct correlation between catalytic performance towards H_2O_2 synthesis and phenol degradation was not observed. With the 0.5% Pd–0.5% Fe/TiO$_2$ catalyst seen to be significantly more active towards phenol degradation (48%) compared to the alternative Pd-based catalysts, including the Pd-only (21%) and PdAu (5%) analogues, despite both these materials displaying H_2O_2 formation rates comparable to or greater than the 1% PdFe/TiO$_2$ catalyst. This is perhaps unsurprising, given the ability

of Fe to catalyse the formation of reactive oxygen species, such as ˙OH, from H_2O_2.[46] Further studies revealed that there is a requirement for both Pd and Fe to be immobilised onto the same grain of support, with the bi-metallic catalyst greatly outperforming a physical mixture of the monometallic analogues (12%).

The significant improvement in phenol degradation in the presence of H_2 and O_2 in comparison to that observed when molecular H_2 (6% phenol conversion) or O_2 (4% phenol conversion) were used alone, or when commercial H_2O_2 (<1% phenol conversion) was used should also be noted (Table S.4†). With the relatively high rate of phenol conversion observed in the presence of a reductive atmosphere alone (5% H_2/CO_2 and N_2) ascribed to the formation of low concentrations of H_2O_2, with dissolved O_2 present in the reaction solution, rather than phenol hydrogenation. While numerous studies have reported the ability of Pd surfaces to catalyse the reduction of phenol to cyclohexanone, typically temperatures far exceeding that used within this work are required.[47] Indeed, our analysis by ^1H NMR (Fig. S.2, ESI†) does not indicate the formation of phenol hydrogenation products, such as cyclohexanol and cyclohexanone.

With the high catalytic efficacy of the 0.5% Pd–0.5% Fe/ TiO$_2$ catalyst established we next investigated the effect of Fe : Pd ratio on phenol degradation activity (Fig. 1). Given the separate and distinct roles of Pd and Fe, with the former primarily catalysing the synthesis of H_2O_2, and the latter subsequently activating the synthesised H_2O_2 through Fenton's pathways to oxygen-centred radicals, which are considered to be the key species responsible for phenol degradation, it is imperative to balance both reactions to achieve maximal oxidant efficiency.

As indicated by our previous studies into the direct synthesis of H_2O_2 under conditions optimised for H_2O_2 stability (Table 1) the addition of Fe, regardless of total content does not significantly alter catalytic activity towards H_2O_2 synthesis under reaction conditions identical to those utilised for the oxidative degradation of phenol, *i.e.*, under near-ambient reaction temperatures and in the absence of the methanol co-solvent (Fig. S.3†). However, with increasing Pd content, activity towards H_2O_2 degradation is seen to decrease substantially (Table S.5†), in keeping with our previous studies into analogous AuPd catalysts.[29] Subsequent

Table 2 Catalytic performance of Pd-based bi-metallic catalysts towards the oxidative degradation of phenol *via* the *in situ* production of H_2O_2

Catalyst	Phenol conversion/%	Selectivity towards phenolic derivatives/%	Selectivity towards organic acids/%
1% Pd/TiO$_2$	11.0	11.0	89.0
0.5% Pd–0.5% Au/TiO$_2$	12.0	10.0	90.0
0.5% Pd–0.5% Cu/TiO$_2$	6.0	6.0	94.0
0.5% Pd–0.5% Co/TiO$_2$	6.0	43.0	57.0
0.5% Pd–0.5% Fe/TiO$_2$	39.0	31.0	69.0
1% Pd/TiO$_2$ + 1% Fe/TiO$_2$[a]	12.0	37.0	63.0

Phenol degradation reaction conditions: catalyst (0.01 g), phenol (1000 ppm, 8.5 g), 5% H_2/CO_2 (420 psi), 25% O_2/CO_2 (160 psi), 2 h, 30 °C, 2 h. [a] The mass of each catalyst is reduced to 0.005 g, to ensure total moles of metal are identical to those in the 0.5% Pd–0.5% Fe/TiO$_2$ catalyst.
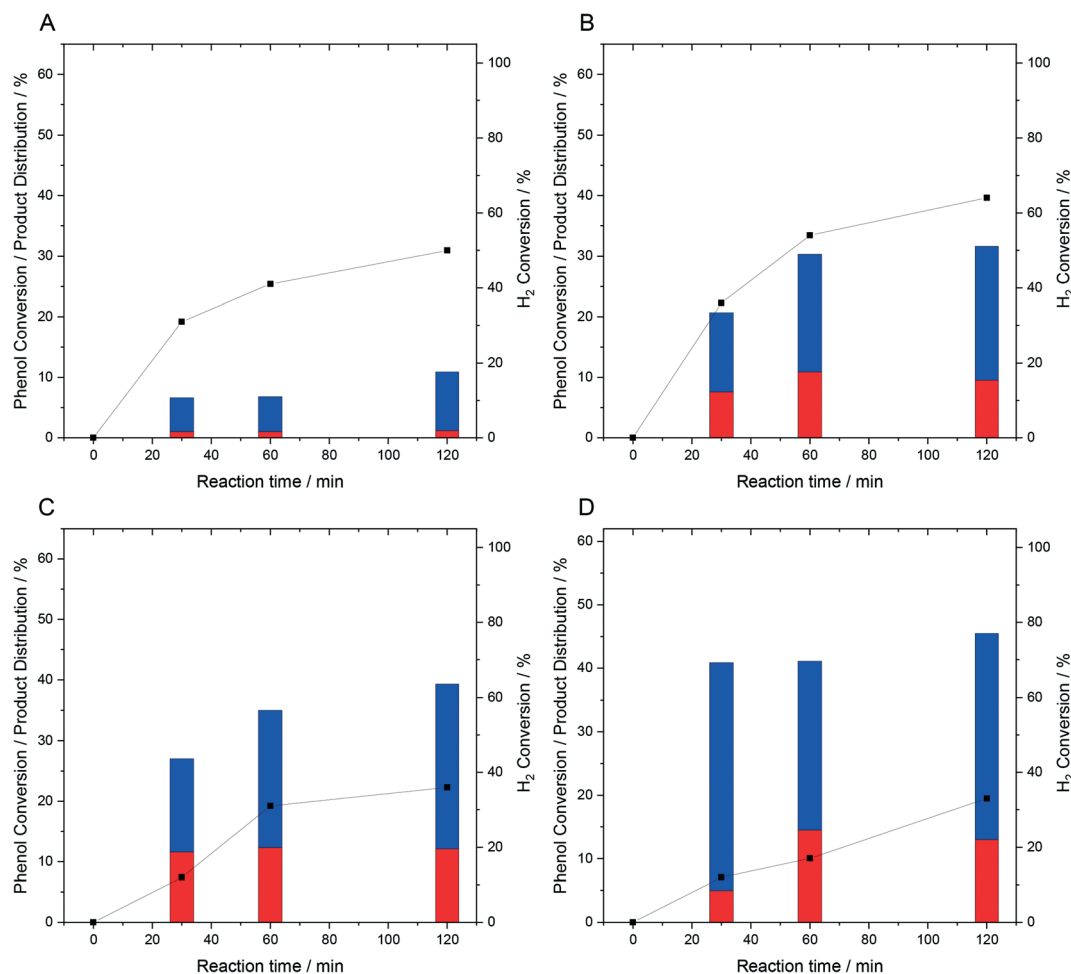
7870 | *Catal. Sci. Technol.*, 2021, **11**, 7866–7874

This journal is © The Royal Society of Chemistry 2021

Fig. 1 Catalytic activity of 1% PdFe/TiO$_2$ catalysts towards the oxidative degradation of phenol, *via in situ* H$_2$O$_2$ production, as a function of Pd : Fe ratio. (A) 1% Pd/TiO$_2$, (B) 0.75% Pd–0.25% Fe/TiO$_2$, (C) 0.5% Pd–0.5% Fe/TiO$_2$ and (D) 0.25% Pd–0.75% Fe/TiO$_2$ phenol degradation reaction conditions: catalyst (0.01 g), phenol (1000 ppm, 8.5 g), 5% H$_2$/CO$_2$ (420 psi), 25% O$_2$/CO$_2$ (160 psi), 2 h, 30 °C. Key; selectivity towards phenolic derivatives (red bar), selectivity towards organic acids (blue bar), H$_2$ conversion (black squares). Note: the activity of the 1% Fe/TiO$_2$ catalyst was found to be within experimental error of the blank reaction.

investigation into the performance of the 1% PdFe/TiO$_2$ catalysts towards the oxidative degradation of phenol revealed an optimal catalyst formulation of 0.25% Pd–0.75% Fe/TiO$_2$, with this catalyst displaying the highest rate of phenol conversion (46%) over a 2 h reaction (Fig. 1).

Analysis of the as-prepared 1% PdFe/TiO$_2$ catalysts by XPS is reported in Fig. S.4.† In the case of the 1% Pd/TiO$_2$ catalyst Pd is seen to exist almost entirely as Pd^0, which may be expected given the reductive heat treatment (4 h, 400 °C, 5%H$_2$/Ar) applied to these materials prior to use. The introduction of Fe was found to result in a clear shift in Pd oxidation state, towards Pd^{2+}, with a strong relationship between Fe content and the proportion of Pd^{2+} observed. Indeed, in the case of the 0.25% Pd–0.75% Fe/TiO$_2$ catalyst Pd was found to exist predominantly as Pd^{2+}. Meanwhile for all bi-metallic catalysts Fe was found to exist primarily as Fe^{2+}, as evidenced by a signal at approximately 709–710 eV and satellite signal at 715 eV. Contrastingly, Fe was found to be present predominantly as Fe^{3+} in the monometallic Fe

catalyst, as evidenced by a signal at 711 eV and a corresponding satellite at approximately 719 eV, although as in the bi-metallic PdFe catalysts some Fe^{2+} is also observed. Given the increased selectivity of domains of mixed Pd oxidation state towards H$_2$O$_2$,[14] it is therefore reasonable to attribute the increased phenol degradation activity of the PdFe catalysts, in part, to an inhibition of competitive H$_2$O$_2$ degradation pathways and improved utilisation of H$_2$O$_2$ in the formation of reactive oxygen species.

With the strong correlation between catalytic selectivity and nanoparticle size well known,[48] we subsequently established the high dispersion of the PdFe nanoparticles, by XRD (Fig. S.5†) and TEM (Fig. S.6†), with no observable nanoparticles detected regardless of Pd : Fe ratio. This is in keeping with our previous work into supported Pd catalysts prepared by an analogous excess chloride procedure, with this route to catalyst synthesis well known to offer improved metal dispersion compared to a conventional wet co-impregnation methodology.[29]

This journal is © The Royal Society of Chemistry 2021

Catal. Sci. Technol., 2021, **11**, 7866–7874 | **7871**

The relatively high H_2 conversion rates observed over the bi-metallic PdFe catalysts at extended reaction times (Fig. 1), in addition to the concurrent plateau in phenol conversion may be indicative of the reaction becoming limited by H_2 availability. This can be understood through the first order dependence of H_2O_2 production with respect to H_2 (ref. 49) and in turn the limited generation of reactive oxygen species, responsible for phenol degradation, when H_2 availability decreases. To determine if this was the case and with a focus on the 0.5% Pd–0.5% Fe/TiO_2 catalyst we next conducted a series of sequential phenol oxidation tests, where the reagent gases were replenished at 2 h intervals (Fig. 2). It is observed that, while it is possible to enhance phenol conversion through replacement of gaseous reagents (67% over four sequential reactions) it is clear that catalytic performance decreases over multiple phenol degradation reactions, possibly indicative of catalyst deactivation rather than limited reagent availability.

For any heterogeneous catalyst operating in a three-phase system the possibility of the leaching of the active phase and resulting homogeneous contribution to observed catalytic performance is of great concern, with the activity of homogeneous Fe and Pd species known to catalyse the formation of oxygen-based radicals (*via* Fenton's pathways) and the direct synthesis of H_2O_2 respectively.[49–53] Analysis of post reaction solutions *via* MP-AES (Table S.6†) reveals minimal leaching of Pd in the post-reaction solution. On the other hand, a significant amount of leached Fe is observed, regardless of catalyst composition. This is in keeping with previous investigations that established the ability of phenolic oxidative products, such as oxalic acid and catechol, to chelate to heterogeneous Fe species and promote their dissolution.[54] With MP-AES analysis of post-reaction solutions in the absence of phenol, or under conditions where H_2O_2 is not generated (Table S.7†), providing further

evidence of the role of phenol oxidation products to promote the leaching of supported metals.

With a particular focus on the 0.5% Pd–0.5% Fe/TiO_2 catalyst, we next conducted a series of hot-filtration experiments to identify the contribution of leached metal species to catalytic activity (Fig. 3). In the absence of the heterogeneous catalyst, minimal additional phenol conversion was observed (41%) after a two-part, 2 h experiment, where the heterogeneous catalyst was removed by filtration after 1 h prior to the post-reaction solution being returned to the reactor for a further 1 h. This value was nearly identical to that observed for the 0.5% Pd–0.5% Fe/TiO_2 catalyst over a 1 h reaction (35%), with the limited additional conversion of phenol possibly attributed to the contribution from residual H_2O_2 generated in the initial 1 h reaction.

To determine if the inactivity observed in the 0.5% Pd–0.5% Fe/TiO_2 catalyst hot-filtration experiment was due to the limited ability of the homogeneous component to synthesize H_2O_2, which may be reasonable given our previous studies which identified the stability of Pd during the phenol degradation reaction (Tables S.6 and S.7†) a further hot-filtration experiment was conducted whereby, after the initial 1 h reaction, the 0.5% Pd–0.5% Fe/TiO_2 catalyst was replaced with a 1% Pd/TiO_2 analogue, ensuring that the total moles of Pd was equal to that in the 0.5% Pd–0.5% Fe/TiO_2 catalyst. Perhaps unexpectedly, given the ability of the 1% Pd/TiO_2 catalyst to catalyse the oxidative degradation of phenol (Fig. 1)
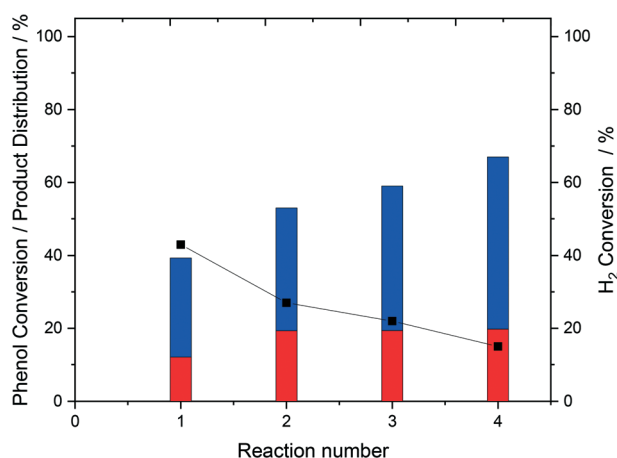

Fig. 2 Comparison of the catalytic activity toward the oxidative degradation of phenol *via in situ* H_2O_2 synthesis over sequential reaction number. Phenol degradation reaction conditions: catalyst (0.01 g), phenol (1000 ppm, 8.5 g), 5% H_2/CO_2 (420 psi), 25% O_2/CO_2 (160 psi), 2 h, 30 °C, 2 h. key; selectivity towards phenolic derivatives (red bar), selectivity towards organic acids (blue bar), H_2 conversion (black squares).
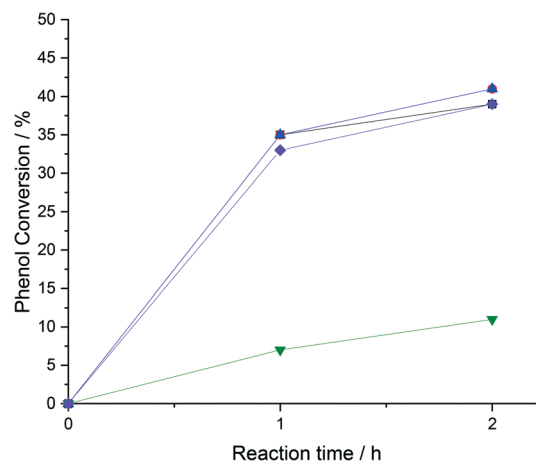

Fig. 3 Efficacy of leached species in oxidative degradation of phenol as identified by a hot filtration experiment using the 0.5% Pd/3% Fe-ZSM-5 catalyst. Phenol oxidation reaction conditions: catalyst (0.01 g), phenol (1000 ppm), 5% H_2/CO_2 (420 psi), 25% O_2/CO_2 (160 psi), 1200 rpm, 2 h, 30 °C. key: 0.5% Pd–0.5% Fe/TiO_2 catalysed reaction (black squares); 1% Pd/TiO_2 catalysed reaction (green inverted triangles); hot filtration reaction where the 0.5% Pd–0.5% Fe/TiO_2 catalyst is removed by filtration after 1 h (red circles); hot filtration reaction where 0.5% Pd–0.5% Fe/TiO_2 catalyst removed by filtration after 1 h and replaced by 1% Pd/TiO_2 catalyst for final 1 h of reaction (blue triangles), hot filtration reaction where 0.5% Pd–0.5% Fe/TiO_2 catalyst removed by filtration after 1 h and replaced by commercial H_2O_2 (concentration identical to that if all H_2 utilised in a standard *in situ* reaction was selectively converted to H_2O_2) catalyst for final 1 h of reaction (purple diamonds).

7872 | *Catal. Sci. Technol.*, 2021, **11**, 7866–7874

This journal is © The Royal Society of Chemistry 2021

an increase in phenol conversion was observed (41%), similar to the sum of the 0.5% Pd–0.5% Fe/TiO₂ (35%) and 1% Pd/TiO₂ (7%) components when they were used independently over 1 h. Indeed, the extent of phenol conversion was found to be nearly identical to that observed over the analogous two-part, 2 h duration experiment conducted over the 0.5% Pd–0.5% Fe/TiO₂ catalyst alone (39%). Given the ability of the 1% Pd/TiO₂ catalyst to promote the degradation of phenol this experiment was unable to confirm a contribution from homogeneous Fe species. In a final experiment, after the initial 1 h reaction utilising the 0.5% Pd–0.5% Fe/TiO₂ catalyst alone, commercial H₂O₂, at a concentration equivalent to if all H₂ in the *in situ* reaction was selectively converted to H₂O₂, was added to the reaction mixture. After a further 1 h reaction (carried out in the presence of an atmosphere of O₂/CO₂ and the absence of a heterogenous catalyst) a small improvement in phenol conversion was observed (39%). When coupled with the known ability of homogenous Fe species to catalyse the formation of oxygen based radical species, *via* the Fenton process, this may be indicative of a homogenous component. However, if there is a homogeneous component to catalytic activity we consider these experiments, in addition to those which illustrate the need for close contact between Pd and Fe species (Table 2), to indicate that such a contribution is minimal.

Conclusion

We have demonstrated that the introduction of Fe into supported Pd catalysts can enhance catalytic performance, not only towards the direct synthesis of H₂O₂ but also the oxidative degradation of phenol *via in situ* H₂O₂ production. This is observed under reaction conditions where conversion is limited when using commercial H₂O₂. The enhanced catalytic performance of the 1% PdFe/TiO₂ catalyst, observed to be almost four times more active than the Pd-only analogue, is attributed to decreased H₂O₂ degradation pathway and the ability of Fe to promote the formation of highly reactive oxygen-based radicals *via* Fenton's pathways. While catalyst stability is still of concern, with substantial leaching of Fe observed, which is promoted by phenol oxidation products observed we consider that these catalysts represent a promising basis for further exploration for the oxidative degradation of a range of recalcitrants.

Conflicts of interest

The authors declare no conflict of interests.

Acknowledgements

References

1 T. A. Larsen, S. Hoffmann, C. Lüthi, B. Truffer and M. Maurer, *Science*, 2016, **352**, 928–933.

2 S. B. Grant, J. Saphores, D. L. Feldman, A. J. Hamilton, T. D. Fletcher, P. L. M. Cook, M. Stewardson, B. F. Sanders, L. A. Levin, R. F. Ambrose, A. Deletic, R. Brown, S. C. Jiang, D. Rosso, W. J. Cooper and I. Marusic, *Science*, 2012, **337**, 681–686.

3 A. Fernandes, P. Makoś, J. A. Khan and G. Boczkaj, *J. Cleaner Prod.*, 2019, **208**, 54–64.

4 S. Esplugas, J. Giménez, S. Contreras, E. Pascual and M. Rodríguez, *Water Res.*, 2002, **36**, 1034–1042.

5 H. J. H. Fenton, *J. Chem. Soc., Trans.*, 1894, **65**, 899–910.

6 F. J. Potter and J. A. Roth, *Hazard. Waste Hazard. Mater.*, 1993, **10**, 151–170.

7 J. A. Zazo, J. A. Casas, A. F. Mohedano, M. A. Gilarranz and J. J. Rodríguez, *Environ. Sci. Technol.*, 2005, **39**, 9295–9302.

8 R. J. Lewis and G. J. Hutchings, *ChemCatChem*, 2019, **11**, 298–308.

9 J. R. Scoville and I. A. Novicova, (Cottrell Ltd.), US 5900256, 1996.

10 Y. T. G. Gao, X. Gong, Z. Pan, K. Yong and B. Zong, *Chin. J. Catal.*, 2020, **41**, 1039–1047.

11 N. M. Wilson and D. W. Flaherty, *J. Am. Chem. Soc.*, 2016, **138**, 574–586.

12 D. W. Flaherty, *ACS Catal.*, 2018, **8**, 1520–1527.

13 R. J. Lewis, K. Ueura, Y. Fukuta, S. J. Freakley, L. Kang, R. Wang, Q. He, J. K. Edwards, D. J. Morgan, Y. Yamamoto and G. J. Hutchings, *ChemCatChem*, 2019, **11**, 1673–1680.

14 X. Gong, R. J. Lewis, S. Zhou, D. J. Morgan, T. E. Davies, X. Liu, C. J. Kiely, B. Zong and G. J. Hutchings, *Catal. Sci. Technol.*, 2020, **10**, 4635–4644.

15 G. Han, X. Xiao, J. Hong, K. Lee, S. Park, J. Ahn, K. Lee and T. Yu, *ACS Appl. Mater. Interfaces*, 2020, **12**, 6328–6335.

16 S. Sterchele, P. Biasi, P. Centomo, P. Canton, S. Campestrini, T. Salmi and M. Zecca, *Appl. Catal., A*, 2013, **468**, 160–174.

17 Q. Liu, J. C. Bauer, R. E. Schaak and J. H. Lunsford, *Appl. Catal., A*, 2008, **339**, 130–136.

18 S. J. Freakley, Q. He, J. H. Harrhy, L. Lu, D. A. Crole, D. J. Morgan, E. N. Ntainjua, J. K. Edwards, A. F. Carley, A. Y. Borisevich, C. J. Kiely and G. J. Hutchings, *Science*, 2016, **351**, 965–968.

19 S. Maity and M. Eswaramoorthy, *J. Mater. Chem. A*, 2016, **4**, 3233–3237.

20 D. A. Crole, R. Underhill, J. K. Edwards, G. Shaw, S. J. Freakley, G. J. Hutchings and R. J. Lewis, *Philos. Trans. R. Soc. London*, 2020, **378**, 20200062.

21 D. Ding, X. Xu, P. Tian, X. Liu, J. Xu and Y.-F. Han, *Chin. J. Catal.*, 2018, **39**, 673–681.

22 K. Cao, H. Yang, S. Bai, Y. Xu, C. Yang, Y. Wu, M. Xie, T. Cheng, Q. Shao and X. Huang, *ACS Catal.*, 2021, **11**, 1106–1118.

This journal is © The Royal Society of Chemistry 2021

Catal. Sci. Technol., 2021, **11**, 7866–7874 | 7873

23 H. Xu, D. Cheng and Y. Gao, *ACS Catal.*, 2017, **7**, 2164–2170.

24 C. M. Crombie, R. J. Lewis, D. Kovačič, D. J. Morgan, T. E. Davies, J. K. Edwards, M. S. Skjøth-Rasmussen and G. J. Hutchings, *Catal. Lett.*, 2021, **151**, 164–171.

25 C. M. Crombie, R. J. Lewis, D. Kovačič, D. J. Morgan, T. J. A. Slater, T. E. Davies, J. K. Edwards, M. S. Skjøth-Rasmussen and G. J. Hutchings, *Catal. Lett.*, 2021, **151**, 2762–2774.

26 R. Underhill, M. Douthwaite, R. J. Lewis, P. J. Miedziak, R. D. Armstrong, D. J. Morgan, S. J. Freakley, T. Davies, A. Folli, D. M. Murphy, Q. He, O. Akdim, J. K. Edwards and G. J. Hutchings, *Res. Chem. Intermed.*, 2021, **47**, 303–324.

27 T. Richards, J. H. Harrhy, R. J. Lewis, A. G. R. Howe, G. M. Suldecki, A. Folli, D. J. Morgan, T. E. Davies, E. J. Loveridge, D. A. Crole, J. K. Edwards, P. Gaskin, C. J. Kiely, Q. He, D. M. Murphy, J.-Y. Maillard, S. J. Freakley and G. J. Hutchings, *Nat. Catal.*, 2021, **4**, 575–585.

28 M. Sankar, Q. He, M. Morad, J. Pritchard, S. J. Freakley, J. K. Edwards, S. H. Taylor, D. J. Morgan, A. F. Carley, D. W. Knight, C. J. Kiely and G. J. Hutchings, *ACS Nano*, 2012, **6**, 6600–6613.

29 A. Santos, R. J. Lewis, G. Malta, A. G. R. Howe, D. J. Morgan, E. Hampton, P. Gaskin and G. J. Hutchings, *Ind. Eng. Chem. Res.*, 2019, **58**, 12623–12631.

30 J. K. Edwards, A. Thomas, A. F. Carley, A. A. Herzing, C. J. Kiely and G. J. Hutchings, *Green Chem.*, 2008, **10**, 388.

31 N. Fairley, V. Fernandez, M. Richard-Plouet, C. Guillot-Deudon, J. Walton, E. Smith, D. Flahaut, M. Greiner, M. Biesinger, S. Tougaard, D. Morgan and J. Baltrusaitis, *Appl. Surf. Sci.*, 2021, **5**, 100112.

32 J. Brehm, R. J. Lewis, D. J. Morgan, T. E. Davies and G. J. Hutchings, *Catal. Lett.*, 2021, DOI: 10.1007/s10562-021-03632-6.

33 N. M. Wilson, P. Priyadarshini, S. Kunz and D. W. Flaherty, *J. Catal.*, 2018, **357**, 163–175.

34 T. García, S. Agouram, A. Dejoz, J. F. Sánchez-Royo, L. Torrente-Murciano and B. Solsona, *Catal. Today*, 2015, **248**, 48–57.

35 R. C. C. Costa, M. F. F. Lelis, L. C. A. Oliveira, J. D. Fabris, J. D. Ardisson, R. R. V. A. Rios, C. N. Silva and R. M. Lago, *J. Hazard. Mater.*, 2006, **129**, 171–178.

36 C. M. Crombie, R. J. Lewis, R. L. Taylor, D. J. Morgan, T. E. Davies, A. Folli, D. M. Murphy, J. K. Edwards, J. Qi, H. Jiang, C. J. Kiely, X. Liu, M. S. Skjøth-Rasmussen and G. J. Hutchings, *ACS Catal.*, 2021, **11**, 2701–2714.

37 L. Ouyang, P. Tian, G. Da, X. Xu, C. Ao, T. Chen, R. Si, J. Xu and Y. Han, *J. Catal.*, 2015, **321**, 70–80.

38 F. Alotaibi, S. Al-Mayman, M. Alotaibi, J. K. Edwards, R. J. Lewis, R. Alotaibi and G. J. Hutchings, *Catal. Lett.*, 2019, **149**, 998–1006.

39 M. H. Ab Rahim, R. D. Armstrong, C. Hammond, N. Dimitratos, S. J. Freakley, M. M. Forde, D. J. Morgan, G. Lalev, R. L. Jenkins, J. A. Lopez-Sanchez, S. H. Taylor and G. J. Hutchings, *Catal. Sci. Technol.*, 2016, **6**, 3410–3418.

40 A. M. Joshi, W. N. Delgass and K. T. Thomson, *J. Phys. Chem. C*, 2007, **111**, 7384–7395.

41 S. Varnagiris, M. Urbonavicius, S. Sakalauskaite, R. Daugelavicius, L. Pranevicius, M. Lelis and D. Milcius, *Sci. Total Environ.*, 2020, **720**, 137600.

42 M. Abidi, A. Hajjaji, A. Bouzaza, K. Trablesi, H. Makhlouf, S. Rtimi, A. A. Assadi and B. Bessais, *J. Photochem. Photobiol., A*, 2020, **400**, 112722.

43 S. Y. Yang, D. Kim and H. Park, *Environ. Sci. Technol.*, 2014, **48**, 2877–2884.

44 F. Mijangos, F. Varona and N. Villota, *Environ. Sci. Technol.*, 2006, **40**, 5538–5543.

45 G. Li, J. Edwards, A. F. Carley and G. J. Hutchings, *Catal. Commun.*, 2007, **8**, 247–250.

46 F. J. Benitez, J. Beltran-Heredia, J. L. Acero and F. J. Rubio, *Ind. Eng. Chem. Res.*, 1999, **38**, 1341–1349.

47 H. Zhou, B. Han, T. Liu, X. Zhong, G. Zhuang and J. Wang, *Green Chem.*, 2017, **19**, 3585–3594.

48 P. Tian, L. Ouyang, X. Xu, C. Ao, X. Xu, R. Si, X. Shen, M. Lin, J. Xu and Y.-F. Han, *J. Catal.*, 2017, **349**, 30–40.

49 Q. Liu and J. H. Lunsford, *Appl. Catal., A*, 2006, **314**, 94–100.

50 V. Kavitha and K. Palanivelu, *Chemosphere*, 2004, **55**, 1235–1243.

51 V. Kavitha and K. Palanivelu, *Int. J. Environ. Sci. Technol.*, 2016, **13**, 927–936.

52 Y. Nomura, T. Ishihara, Y. Hata, K. Kitawaki, K. Kaneko and H. Matsumoto, *ChemSusChem*, 2008, **1**, 619–621.

53 S. J. Freakley, N. Agarwal, R. U. McVicker, S. Althahban, R. J. Lewis, D. J. Morgan, N. Dimitratos, C. J. Kiely and G. J. Hutchings, *Catal. Sci. Technol.*, 2020, **10**, 5935–5944.

54 S. O. Lee, T. Tran, Y. Y. Park, S. J. Kim and M. J. Kim, *Int. J. Miner. Process.*, 2006, **80**, 144–152.

7874 | *Catal. Sci. Technol.*, 2021, **11**, 7866–7874

This journal is © The Royal Society of Chemistry 2021